Spectroscopic investigation of the deeply buried Cu(In,Ga)(S,Se)$_2$/Mo interface in thin-film solar cells

L. Weinhardt,[a] O. Fuchs, A. Peter, and E. Umbach
Experimentelle Physik II, Universität Würzburg, Am Hubland, 97074 Würzburg, Germany

C. Heske[b]
Department of Chemistry, University of Nevada, Las Vegas, Nevada 89154

J. Reichardt,[c] M. Bär,[d] I. Lauermann, I. Kötschau, A. Grimm,
S. Sokoll, and M. Ch. Lux-Steiner[e]
Department SE 2, Hahn-Meitner-Institut, Glienicker Straße 100, 14109 Berlin, Germany

T. P. Niesen, S. Visbeck, and F. Karg
Shell Solar, D-81739 Munich, Germany

The Cu(In,Ga)(S,Se)$_2$/Mo interface in thin-film solar cells has been investigated by surface-sensitive photoelectron spectroscopy, bulk-sensitive x-ray emission spectroscopy, and atomic force microscopy. It is possible to access this deeply buried interface by using a suitable lift-off technique, which allows us to investigate the back side of the absorber layer as well as the front side of the Mo back contact. We find a layer of Mo(S,Se)$_2$ on the surface of the Mo back contact and a copper-poor stoichiometry at the back side of the Cu(In,Ga)(S,Se)$_2$ absorber. Furthermore, we observe that the Na content at the Cu(In,Ga)(S,Se)$_2$/Mo interface as well as at the inner grain boundaries in the back contact region is significantly lower than at the absorber front surface. © *2006 American Institute of Physics*. [DOI: 10.1063/1.2168443]

Solar cells based on Cu(In,Ga)(S,Se)$_2$ (CIGSSe) as absorber material belong to the most promising thin-film solar cell technologies. High conversion efficiencies can be reached both on a laboratory scale [19.5% (Ref. 1)] and on large areas [3459 cm^2, 13.4% (Ref. 1)]. The CIGSSe thin-film solar cell is a multilayer structure consisting of the CIGSSe absorber, a ZnO window layer, which is in most cases separated from the absorber by a CdS buffer layer, and the back contact. Today the latter consists of Mo in nearly all cases. In the beginning of the development of CIGSSe solar cells Au was used as a back contact, but later Mo was chosen because of lower costs with no loss in efficiency. Only recently Orgassa *et al.* have made a new attempt of trying alternative back contact materials (W, Ta, Nb, Cr, V, Ti, and Mn), in some cases with very promising results.[2] One main demand for the back contact is a low series resistance, and usually an Ohmic contact to the absorber layer is believed to be optimal. For the CIGSSe/Mo interface some authors find an Ohmic contact[3–5] whereas others find a Schottky barrier.[6,7] One of the main reasons for this discrepancy is that it is difficult to investigate the real CIGSSe/Mo interface as it is found in the cell device. The formation of this interface takes place in parallel to the absorber fabrication and cannot

be viewed as finished until the absorber is completed. Therefore the experiments described in the literature have been performed either on idealized systems (CuInSe$_2$ single crystal and evaporated Mo)[3,7] or by using indirect techniques.[4–6] However, the real CIGSSe/Mo interface is probably much more complicated than can be assessed by such approaches. In particular, it is a challenge to investigate the chemical and electronic properties of thin deeply buried interfaces by surface-sensitive techniques. Thus, there is little information yet available, but it has been found or suggested by several groups that a layer of MoSe$_2$ can exist between absorber and back contact.[4,8,9] Kohara *et al.* even suspected this layer to be responsible for an Ohmic contact at the CIGSSe/Mo interface.[4]

The properties of the Mo back contact—and thus also of the CIGSSe/Mo interface—result from a complex interplay of different factors. These are the directly accessible deposition parameters of the Mo back contact, which have been found to influence the conductivity and the adhesion on the substrate,[10] as well as the less accessible parameters such as the concentration of sodium stemming from the glass substrate or a precursor. For example, a relation between the Na content in the Mo back contact and the formation of the MoSe$_2$ layer has been found.[4] Possibly a diffusion of Mo into the absorber film, which was found for evaporated Mo on CuInSe$_2$ films with temperatures similar to those used during absorber fabrication,[11] might also play a role.

Until today the optimization of the back contact and even the choice of the used material have been done empirically. This is mainly because a detailed investigation of the

---

[a] Electronic mail: lothar.weinhardt@physik.uni-wuerzburg.de
[b] Electronic mail: heske@unlv.nevada.edu
[c] Present address: Institute of Theoretical Physics, Universität Bremen, Otto-Hahn-Allee, 28359 Bremen, Germany.
[d] Present address: Department of Chemistry, University of Nevada, Las Vegas, Nevada 89154.
[e] Also at Freie Universität Berlin, 14195 Berlin, Germany.

properties of the back contact and its interface to the absorber is difficult, as mentioned above. A possible way to investigate this interface nevertheless, is to lift the absorber off the back contact as it was done before by Schmid *et al.*[12] and Scheer and Lewerenz[13] and is followed in this paper to access the real CIGSSe/Mo interface in optimized CIGSSe thin film solar cells. With this approach, a spectroscopic investigation of the real CIGSSe/Mo interface using x-ray photoelectron spectroscopy (XPS), x-ray emission spectroscopy (XES), and atomic force microscopy (AFM) is possible.

All samples were taken directly from the Shell Solar pilot line process (for details see Ref. 14 and references therein). In this process, the Mo back contact is sputtered on a soda-lime glass, which is coated with a Na diffusion barrier. The CIGSSe absorber is then prepared by depositing elemental layers and a Na-containing precursor followed by rapid thermal annealing in a sulfur-containing atmosphere. Then, a CdS buffer layer is added by a standard chemical bath deposition process. Finally a ZnO window layer, which consists of an *i*-ZnO and an *n*-doped ZnO layer, is deposited by sputtering. For the investigation of the CIGSSe/Mo interface, two sample sets were prepared for the XPS and the XES measurements, respectively. The samples were glued with their absorber or window layer front side to a piece of glass using an ultrahigh-vacuum- (UHV) compatible epoxy glue. Then, the front part of the cell was lifted off the back contact, hoping that the cleavage occurs right at the CIGSSe/Mo interface. As will be discussed below, this "hope" is experimentally well justified. For the XPS measurements the cleavage was done in a glovebox under N_2 atmosphere, and immediately afterwards the samples were transferred into UHV to avoid contamination of the cleavage planes. For the XES and AFM experiments, the samples were prepared in air, since for these measurements a few layers of adsorbates do not matter. In the following, the two cleavage planes will be called the "Mo side" and the "CIGSSe back side," respectively. For a comparison, also a pure absorber (without a ZnO window and CdS buffer) was investigated (henceforth called "CIGSSe front side"). For the comparison of this surface with the cleavage planes, surface contamination caused by the air exposure of the pure absorber was removed by mild sputtering with low-energy Ar^+ ions (50 eV, 50 nA/cm^2) for 30 min. While it is well known that prolonged sputtering of CIGSSe with 500 eV Ar^+ leads to the formation of metallic In and Cu (Refs. 15 and 16) and of a Fermi edge,[17,18] we did not find any evidence for such effects when using 50 eV Ar^+.

For the XPS measurements, Mg $K\alpha$ excitation and a VG CLAM 4 electron analyzer were used. The transmission function of the analyzer was determined with reference spectra from Ref. 19 and follows an inverse square-root dependence of the kinetic energy in the relevant energy range. For the quantitative evaluation of element ratios, this transmission function and photoionization cross sections from Ref. 20 were used; for the inelastic mean free path, $\lambda \propto \sqrt{E_{kin}}$ was assumed. The XES spectra were taken at the SXF end station of beamline 8.0 at the Advanced Light Source, Berkeley, CA. Supporting XES experiments were performed with the
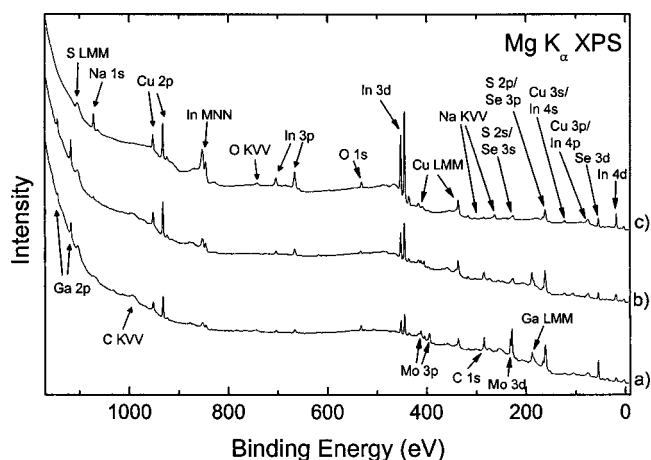

FIG. 1. XPS survey spectra of (a) the "Mo side" and (b) the " CIGSSe back side" after cleavage of a CIGSSe/Mo interface, as well as (c) the "CIGSSe front side" of a CIGSSe absorber after 50 eV Ar$^+$-ion cleaning.

CISSY end station at the BESSY Synchrotron Light Source, Berlin, using the U41-PGM undulator beamline. The base pressure for the XPS measurements was 2×10^{-10} mbar and that for the XES measurements 1×10^{-9} mbar. AFM measurements were performed under ambient conditions with a Topometrix Explorer microscope in noncontact mode.

We first discuss the result of the cleavage preparation, in particular, the question whether the cleavage plane is located at the CIGSSe/Mo interface as desired. The XPS survey spectra in Fig. 1 reveal a wealth of information. First, they show that, due to the N_2 atmosphere used during sample preparation, both cleavage surfaces contain only trace amounts of adsorbed oxygen. The higher amount of carbon is therefore most likely attributed to carbon impurities inside the film. Note that equal concentrations of O and C would result in an O:C peak ratio of 2.9 when taking the cross sections, analyzer transmission, and electron mean free paths into account. Second, since XPS is a very surface-sensitive technique (information depth of a few nanometers), and since the Mo 3d double peak at a binding energy of ~230 eV can only be seen in the survey spectrum of the Mo side [Fig. 1(a)] but not in that of the CIGSSe back side [Fig. 1(b), the structure at similar energy is due to S 2s and Se 3s], we derive that the cleavage plane lies at (or at least very close to) the CIGSSe/Mo interface. This is confirmed by the Mo $M_{4,5}$ XES signal (not shown) which can only be observed on the Mo side.

Thirdly, XPS lines of the absorber elements can be detected on all samples, which suggests that some absorber material also remains on the Mo side. There are now two extreme "scenarios:" one, that only a fraction of the Mo side is covered by crystallites of the absorber film and the rest is uncovered, and the other, that a very thin absorber film (<1 nm, derived by taking the peak intensities into account) covers the entire Mo side. The first scenario sounds much more reasonable since the cohesion at grain boundaries can be expected to be much lower than inside the grains. By comparing with a cleaned Mo reference sample the two different scenarios can be distinguished by the attenuation behavior of the Mo lines. If there was a thin homogeneous
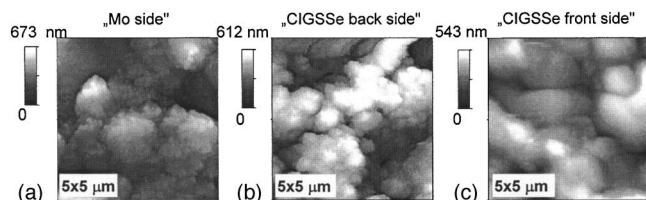
FIG. 2. AFM images of (a) the "Mo side," (b) the "CIGSSe back side," and (c) the "CIGSSe front side" obtained using the noncontact mode. While the two surfaces from the back interface have a small-grained structure, the "CIGSSe front side" shows the typical CIGSSe grain size of around 1 μm.

absorber film covering the Mo side, two Mo-related lines with different kinetic energies (here, Mo $M_{45}VV$ with $E_{kin} \approx 223$ eV and Mo 3d with $E_{kin} \approx 1024$ eV) and therefore different attenuation lengths (for Mo $M_{45}VV$ $\lambda \approx 0.8$ nm and for Mo 3d $\lambda \approx 1.7$ nm) would be attenuated differently. This would give a different intensity ratio of the two lines for the Mo side of the cleaved sample compared to the clean Mo reference sample (e.g., for a film of 1 nm in thickness this ratio should change by a factor of 1.9). However, the ratio between Mo $M_{45}VV$ and Mo 3d of the Mo side is the same as that of the Mo reference, which clearly favors the first scenario, where some absorber crystallites remain at the Mo front side.

It is known from transmission electron microscopy (TEM) measurements that the back part of the Shell Solar absorber consists of small grains, whereas in the front part large grains are found.[8] This is confirmed by the AFM measurements shown in Fig. 2. The CIGSSe front side shows large grains with a size of around 1 μm, whereas the grains at the CIGSSe back side are much smaller. As expected from the XPS results in the preceding paragraph, the AFM picture of the Mo side is very similar to that of the CIGSSe back side. There is strong evidence that the CIGSSe crystallites found on the Mo side stem only from this small-grained part at the back side of the absorber and that all large grains from the absorber front side remain on the CIGSSe side of the cleavage. This is not only based on the AFM measurements in Fig. 2 but also supported by the bulk-sensitive XES measurements (attenuation length around 70 nm) which do not show any Cd $M_{4,5}$ XES emission from the buffer layer. If substantial parts of the absorber (some of the large grains) were left on the Mo side, such emission from the CdS buffer would have been found either on the CIGSSe back side or on the Mo side which is not the case here (note that the XPS spectra of the cleavage planes, which sample a much larger area, show minor amounts of Cd, which can be neglected in the following).

By comparing the line intensities of the absorber elements on the CIGSSe back side and the Mo side, the coverage (surface fraction) of the Mo side by small CIGSSe crystallites can be determined. The Cu, Ga, and In lines yield very similar values [43(±3)%] for the area coverage, i.e., less than half of the Mo side is covered by CIGSSe crystallites. For S and Se the situation is different. As the Se 3d line intensity in the survey spectra of Fig. 1 shows, the Se content is higher at the Mo side than at the CIGSSe back side (and at the CIGSSe front side). This is also visible in the detailed
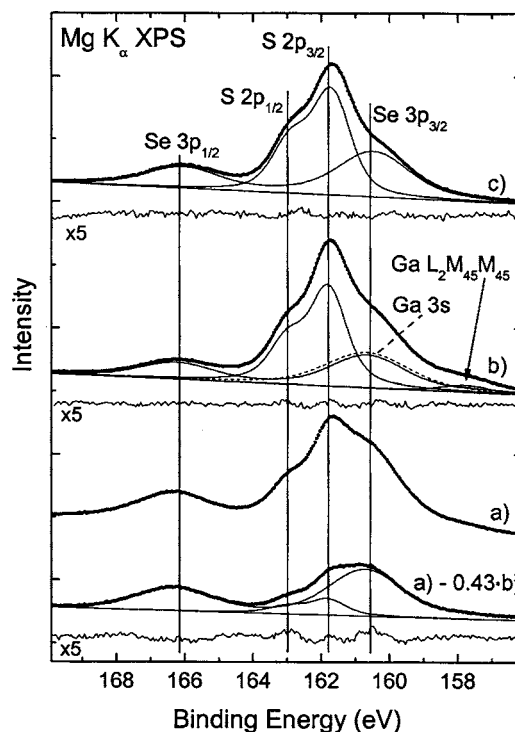

FIG. 3. Detailed XPS spectra of (a) the "Mo side," (b) the "CIGSSe back side," and (c) the "CIGSSe front side." Spectrum (a) is also shown (bottom) after subtracting a fraction of 0.43 of spectrum (b), then representing MoS_2 and $MoSe_2$. The thin lines represent the fits of the spectra, for which also magnified residua are shown.

spectra in Fig. 3, where the Se 3p, S 2p, and, if present, Ga 3s, and Ga $L_2M_{45}M_{45}$ lines are displayed. The S 2p lines indicate that also the S content is higher than expected from the CIGSSe crystallites on the Mo side. This is visualized by subtracting a fraction of 0.43 of the spectrum of the CIGSSe back side (b) from the spectrum of the Mo side (a). The resulting spectrum then can be attributed to S and Se and diffused into the Mo back contact. The XPS peak positions are in agreement with the formation of MoS_2 and $MoSe_2$.[21] For a better visualization and a quantification of the different spectral components fits are shown in Fig. 3, for which peaks with a Voigt line shape and a linear background were used. For the spin-orbit-split peaks, the widths of the two components were coupled and their splitting (1.2 eV for S 2p and 5.6 eV for Se 3p) and intensity ratios [$I(p_{3/2}):I(p_{1/2})=2$] were kept constant.

In accordance with Refs. 4, 8, and 9, we thus find a formation of $MoSe_2$ and MoS_2 at the back interface. The formation of MoS_2 can be further directly verified by the S $L_{2,3}$ XES spectra of the Mo side (a) and the CIGSSe back side (b) displayed in Fig. 4. XES spectra provide detailed information about the local chemical bonding of the S atoms.[22,23] The spectrum of the CIGSSe front side shown in Fig. 4(c) consists of the dominating S $3s \rightarrow$ S 2p transitions labeled (1) and of the emission from the upper valence band filling the 2p holes, where transitions from In 5s- and Ga 4s-derived states labeled (2) and Cu 3d-derived states labeled (3) are visible. The spectrum of the CIGSSe back side in Fig. 4(b) very closely resembles that of the CIGSSe front side with the exception that the features (2) exhibit a differ-
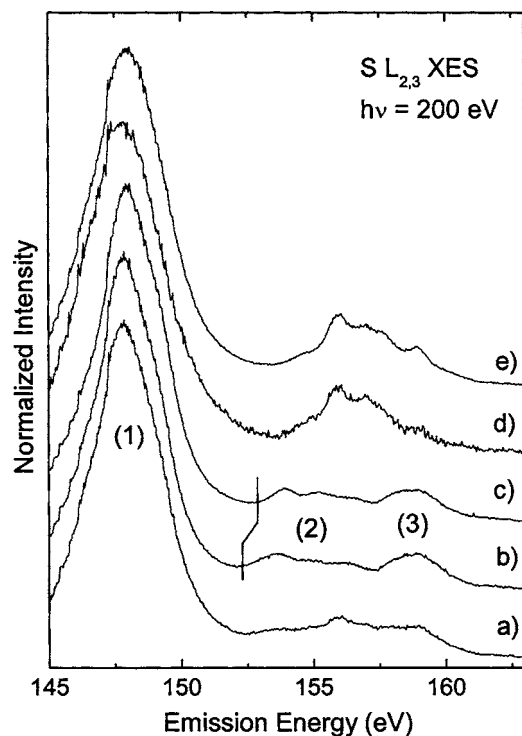
FIG. 4. S $L_{2,3}$ XES spectra of (a) the "Mo side," (b) the "CIGSSe back side," and (c) the "CIGSSe front side." In (d), a fraction of 0.65 of spectrum (b) has been subtracted from spectrum (a). This spectrum very closely resembles the spectrum of a MoS_2 reference sample shown in (e). The structures labeled (1)–(3) are discussed in the text.

ent spectral shape and extend to lower emission energies. Since Ga can be found only at the back side of the absorber (see Figs. 1 and 3 and discussion below), the emission at the low-energy side of structure (2) can be ascribed to the transitions from Ga $4s$-derived states, which in $CuGaS_2$ extend to higher binding energies than the In $5s$-derived states in $CuInS_2$, as band-structure calculations show.[24]

The region of the upper valence band in the spectrum of the Mo side in Fig. 4(a) differs significantly from the corresponding energy range of the spectrum of CIGSSe. This results from a superposition of spectral intensity from grains which are equivalent to those at the CIGSSe back side and of intensity from MoS_2, as proven by spectrum (d) in Fig. 4. For this spectrum, a suitable amount (65%) of the spectrum of the CIGSSe back side (b) was subtracted from that of the Mo side (a), resulting in a spectrum which can be attributed to MoS_2. This is most directly shown by a comparison with the spectrum of a MoS_2 reference sample in Fig. 4(e). Note that S $L_{2,3}$ XES spectra are particularly well suited to derive the chemical environment of the probed atomic species. For Se, this is not the case, and hence a similarly direct proof cannot be given for $MoSe_2$. Nevertheless, based on the photoemission results presented above, it appears safe to infer the formation of $MoSe_2$ as well. This is consistent with a (S+Se):Mo ratio of 2.2, compatible with MoS_2 and $MoSe_2$. This value is derived from the S $2p$ and Se $3p$ intensities attributed to the S and Se diffused into the Mo back contact [bottom spectrum in Fig. 3(a)] and the Mo $3d$ intensity.

Moreover, from this spectrum a $MoSe_2 : MoS_2$ ratio of 2.0 can be derived, corresponding to the formation of a $Mo(S_{0.33}, Se_{0.67})_2$ layer.

The successful cleavage at the absorber/back contact interface now also allows the following comparison of the back side of the absorber with its front surface. The survey spectra in Fig. 1 reveal that Ga is only found at the CIGSSe back side and not at the CIGSSe front side. This is in accordance with earlier measurements that showed that Ga is located near the back contact of the absorber.[8,25] In parallel to the presence of Ga at the CIGSSe back side, the intensity of the In lines is reduced, as expected. A quantitative evaluation of the line intensities of the In $3d$ and Ga $2p$ detailed spectra (not shown) yields an In:Ga ratio of approximately 1.3 at the back side of the absorber. As known from earlier measurements, the S content of the CIGSSe absorber from Shell Solar shows a nonuniform depth distribution where S is found predominantly at the back and at the front side of the absorber.[13,25] Consistent with this finding, a S signal can be found both on the CIGSSe front side and the CIGSSe back side, as seen in Fig. 3. A quantitative evaluation of the line intensities reveals a slightly higher S:Se ratio of 3.1 at the CIGSSe back side compared to 2.7 at the CIGSSe front side.

Evaluating the overall stoichiometry, we find both the CIGSSe front side and the CIGSSe back side to be copper poor with Cu:In ratios of 0.4 and 0.5, respectively. Whereas the copper-poor stoichiometry of the absorber surface is well known for the Shell Solar absorbers[16,17] and for other optimized CIGSSe absorbers,[26–28] to our knowledge this was found only once before at the back side of a $CuInSe_2$ absorber[12], probably due to the difficulty of preparing suitable samples as mentioned above.

Regarding the Na content, a large difference between the CIGSSe front side and the two cleavage planes is found, as revealed by the Na $1s$ peak at a binding energy of 1072 eV in Fig. 1. The integral Na content obtained from detailed (and normalized) spectra (not shown) is 11% for the CIGSSe back side and 4.3% for the Mo side, respectively, compared to the Na content at the CIGSSe front side (100%). This finding will be discussed in the following. As shown above, some absorber crystallites remain at the Mo side. As a result, the spectrum of the CIGSSe back side consists of contributions from the CIGSSe/back contact interface and from inner grain boundaries. In an analogous way, the spectrum of the Mo side stems from the interface and, wherever a crystallite from the absorber remains, from inner grain boundaries of the absorber. Now we can give upper limits for both the Na content at the back interface and that at the inner grain boundaries near the back contact. For doing so, we neglect any attenuation effects, assuming that the depth dependencies of the Na content at the investigated surfaces are similar. It is now assumed that the entire Na signal stems either from the back interface (area fraction of 57%—see above) and not at all from the inner grain boundaries (area fraction of 43%), or vice versa. In the first case we get an upper limit of 27% [(11+4.3)/0.57] of the Na content at the CIGSSe/Mo interface with respect to the CIGSSe front side. Of course the lower limit is zero since the entire Na could be located at the inner grain boundaries. In this latter case, Na should still be

seen on both sides of the interface (of course not necessarily in equal amounts) because of the crystallites attached to the back contact. We then get an upper limit of 36% [(11 +4.3)/0.43] for the Na content at the inner grain boundaries near the back contact with respect to the CIGSSe front side. This result can be correlated to earlier measurements showing that the Na content at the absorber front surface is at least by a factor of 10 larger than that at the inner grain boundaries near the absorber front surface.[29]

In summary, we were able to investigate the deeply buried CIGSSe/Mo interface with surface- and bulk-sensitive techniques by using a suitable lift-off technique for sample preparation. We find a layer of $Mo(S,Se)_2$ on the Mo back contact. Together with the finding of a Cu-poor stoichiometry at the back side of the CIGSSe absorber, this will play a central role for establishing a correct energy-level diagram at the back interface and consequently for answering the question "Schottky barrier versus Ohmic contact," which remains to be investigated in the future. Taking advantage of the finding that some absorber crystallites remain at the Mo side after cleavage, we are able to give an upper limit for the Na content not only at the back interface but also at the inner grain boundaries near this interface. The results show that this Na content is much lower than that at the front surface of the absorber.

[1] M. A. Green, K. Emery, D. L. King, S. Igari, and W. Warta, Prog. Photovoltaics **13**, 49 (2005).

[2] K. Orgassa, H. W. Schock, and J. H. Werner, Thin Solid Films **431–432**, 387 (2003).

[3] A. J. Nelson, D. Niles, L. L. Kazmerski, D. Rioux, R. Patel, and H. Höchst, J. Appl. Phys. **72**, 976 (1992).

[4] N. Kohara, S. Nishiwaki, Y. Hashimoto, T. Negami, and T. Wada, Sol. Energy Mater. Sol. Cells **67**, 209 (2001).

[5] W. N. Shafarman and J. E. Phillips, Proceedings of the 25th IEEE Photovoltaic Specialists Conference, Washington, DC, 1996 (unpublished), p. 917.

[6] P. E. Russell, O. Jamjoum, R. K. Ahrenkiel, L. L. Kazmerski, R. A. Mickelsen, and W. S. Chen, Appl. Phys. Lett. **40**, 995 (1982).

[7] W. Jaegermann, T. Löher, and C. Pettenkofer, Cryst. Res. Technol. **31**, 273 (1996).

[8] V. Probst, W. Stetter, W. Riedel *et al.*, Thin Solid Films **387**, 262 (2001).

[9] Th. Glatzel, D. Fuertes Marron, Th. Schedel-Niedrig, S. Sadewasser, and M. Ch. Lux-Steiner, Appl. Phys. Lett. **81**, 2017 (2002).

[10] J. H. Scofield, A. Duda, D. Albin, B. L. Ballard, and P. K. Predecki, Thin Solid Films **260**, 26 (1995).

[11] T. D. Dzhafarov, M. S. Sadigov, E. Cingi, E. Bacaksiz, and M. Caliskan, J. Mater. Sci. Lett. **19**, 1521 (2000).

[12] D. Schmid, J. Kessler, and H. W. Schock, *Proceedings of the 12th European Photovoltaic Solar Energy Conference*, Amsterdam, 1994 (unpublished), p. 653.

[13] R. Scheer and H.-J. Lewerenz, J. Vac. Sci. Technol. A **13**, 1924 (1995).

[14] J. Palm, V. Probst, A. Brummer *et al.*, Thin Solid Films **431–432**, 514 (2003).

[15] D. W. Niles, K. Ramanathan, F. Hasoon, R. Noufi, B. J. Tielsch, and J. E. Fulghum, J. Vac. Sci. Technol. A **15**, 3044 (1997).

[16] L. Weinhardt, M. Morkel, Th. Gleim, S. Zweigart, T. P. Niesen, F. Karg, C. Heske, and E. Umbach, Proceedings of the 17th EPSEC, Munich, Germany, 2001 (unpublished), p. 1261.

[17] C. Heske, R. Fink, E. Umbach, W. Riedl, and F. Karg, Cryst. Res. Technol. **31**, 919 (1996).

[18] M. Morkel, L. Weinhardt, B. Lohmüller, C. Heske, E. Umbach, W. Riedl, S. Zweigart, and F. Karg, Appl. Phys. Lett. **79**, 4482 (2001).

[19] M. P. Seah and G. C. Smith, Surf. Interface Anal. **15**, 751 (1990).

[20] J. J. Yeh and I. Lindau, At. Data Nucl. Data Tables **32**, 1 (1985).

[21] *Handbook of X-Ray Photoelectron Spectroscopy*, edited by J. F. Moulder, W. F. Stickle, P. E. Sobol, K. D. Bomben, and J. Chastain (Perkin-Elmer Corporation, Eden Prairie, 1992).

[22] C. Heske, U. Groh, O. Fuchs *et al.*, Phys. Status Solidi A **187**, 13 (2001).

[23] C. Heske, U. Groh, L. Weinhardt *et al.*, Appl. Phys. Lett. **81**, 4550 (2002).

[24] J. E. Jaffe and A. Zunger, Phys. Rev. B **28**, 5822 (1983).

[25] M. Bär, W. Bohne, J. Röhrich, E. Strub, S. Lindner, M. C. Lux-Steiner, Ch.-H. Fischer, T. P. Niesen, and F. Karg, J. Appl. Phys. **96**, 3857 (2004).

[26] D. Schmid, M. Ruckh, F. Grunwald, and H. W. Schock, J. Appl. Phys. **73**, 2902 (1993).

[27] T. Dullweber, G. Hanna, U. Rau, and H. W. Schock, Sol. Energy Mater. Sol. Cells **67**, 145 (2001).

[28] J. A. M. AbuShama, S. Johnston, T. Moriarty, G. Teeter, K. Ramanathan, and R. Noufi, Prog. Photovoltaics **12**, 39 (2004).

[29] C. Heske, D. Eich, R. Fink *et al.*, Surf. Interface Anal. **30**, 459 (2000).